JOURNAL OF MATERIALS SCIENCE 27 (1992) 2019–2025

Low-cycle fatigue crack advance and life prediction

YONG JUN OH, SOO WOO NAM
Department of Materials Science Engineering, Korea Advanced Institute of Science Technology, PO Box 150, Cheongryang, Seoul, Korea

A new concept for a fatigue process zone within which the actual degradation of the material takes place is proposed. This zone is described as the region in which the stress distribution of the HRR field approaches the maximum flow stress of the material, with the strain localization caused by a sliding-off process. In high-strain low-cycle fatigue conditions, this new concept is shown to be more realistic for the prediction of the fatigue life than that of previous work which has been based on a rough approximation. The proposed feature of the zone is experimentally supported by microhardness measurements. In particular, although this zone is formulated from continuum mechanics, it reflects microstructural factors such as precipitates and stacking-fault energy. Using the developed fatigue process zone and strain intensification in the zone near the crack tip, a modified analytical model for prediction of the continuous low-cycle fatigue life is proposed. The exponent of the Coffin–Manson law obtained from the present prediction is suggested to be $1/(3n' + 1)$, which is different from the previously reported value of $1/(2n' + 1)$, and is shown to be in good agreement with experimental results for five alloy systems.

1. Introduction

It is well known that, in the fatigue crack tip region, there is a process zone within which the actual degradation process takes place during crack propagation. Generally, the form of degradation is different from one material to another such as micro-cracking, void formation or shearing bands. In the low-cycle fatigue (LCF) condition, it has been reported that the crack advance of a ductile material is preceded by localized plastic deformation [1–8]. This type of deformation takes the form of narrow shear bands which sustain large shear strains. In this respect, by considering the crack tip stress and strain distribution from a macroscopic viewpoint and the dislocation behaviour near the crack tip from a microscopic viewpoint, many authors have developed models for LCF crack advance and the endurance [8–12].

Tomkins and Wareing [3] have proposed that the crack advance is determined by the amount of sliding-off in the crack tip deformation bands, and the size of such bands is obtained from an approximation of the Dugdale model for the plastic zone size. Yokobori *et al.* [10] have proposed that the fatigue crack propagation rate depends on the number of dislocations emitted from the crack tip in an appropriate length (or process zone), s, and the size of the process zone can be obtained from a simple approximation for the plastic zone size. However, even though life predictions were successful, these models were based on a rough approximation for the extent of the crack tip process zone (shearing zone) such as the LEFM assumption. Therefore, these models can be considered to be insufficient to represent the precise features of the process zone.

Meanwhile, there have been some models to correlate the process zone with metallurgical factors. According to the model of Saxena and Antolovich's [13], the LCF process is assumed to occur in some region l ahead of the main crack and the crack advances l units in ΔN cycles, where ΔN represents the number of cycles to crack initiation for an average plastic strain range $\Delta\varepsilon_p$ in the process zone. From this assumption, an equation containing a term in l was obtained for the crack advance and correlations of the zone with microstructural factors were suggested. Also, Davidson [14] has developed a model for the fatigue crack advance at near-threshold rates based on dislocation sliding-off over a length of slip line r_s (which can be considered as the process zone), and correlated the length of the slip line with metallurgical and mechanical parameters. However, the authors of these two models have reversely determined the process zone size from the crack growth rate equations, and the physical correlations between the process zone size and metallurgical and mechanical factors were not represented in their equation. That is, the proposed models are considered to be not formulated from an adequate explanation for the process zone itself.

Generally, in high strain and temperature ranges, it is well known that the stress and strain distribution of the J-field is prevalent instead of a K-field near the crack tip region. Likewise, this field may be considered to be effective in the situation of an LCF crack. Therefore, in this work, on the basis of the stress and

0022–2461

strain distribution of the J-field ahead of the crack tip, a concept concerning the process zone in high-strain LCF is introduced for the development of a new model. Since the intensified average strain in the zone is considered, a model for LCF life prediction is developed based on the concept of crack growth by crack tip sliding-off. In the present model, the factors for high fatigue resistance are discussed in terms of the concepts for the process zone and intensified strain in the zone. In particular, the correlations of these factors with microstructural characteristics will be taken into account.

2. Model development

Observing the characteristic features of fatigue crack tips using micro-hardness tests [10, 13, 15, 16], electro-channeling methods [17] and etching techniques [18], many investigators identified that the region ahead of the fatigue crack is parabolically hardened as a result of the intensified deformation during repeated cycling under the influence of the crack tip stress field. Generally, this region is called the cyclic plastic zone. However, in the region closer to the tip there exists a fatigue process zone within which the actual process of material degradation takes place during crack propagation. In general, what is happening in such a process zone is considered as a shearing decohesion or void formation caused by severe local shearing processes in ductile materials. In this process zone, the distribution of stress and strain is not clearly defined yet in a singular form. Nevertheless, based on the idea that the area of the process zone is nearly at the point of the fracture, Tomkins [8] and Jaske [19] have assumed in their models that the stress level in the crack tip process zone approaches the ultimate tensile strength of previously cycled material.

The nature of the deformation in the crack-tip region can be identified by microhardness measurements ahead of the fatigue crack tip. Fig. 1 shows the experimentally measured microhardness profile adjacent to the fatigue crack tip for 304L stainless steel. (Detailed experimental procedures are reported in the next section.) It is found to be consistent with Jaske's description [19] for the crack tip flow stress distribution. A monotonically hardened region, independent of the crack tip stress field, is characterized by a nearly constant microhardness while it increases parabolically in the cyclic plastic zone as a result of crack tip stress intensification.

According to Rice [20], the distance of the cyclic plastic zone boundary, r_f, from the crack tip, i.e. the distance between the crack tip and the first increasing point of the monotonic flow stress, can be given by

$$r_f = \alpha' \left(\frac{\Delta K}{2\sigma_{yc}}\right)^2 = \alpha_f \left(\frac{\sigma_T}{\sigma_{yc}}\right)^2 a \qquad (1)$$

where α' and α_f are constants, σ_T and σ_{yc} are the tensile peak stress and cyclic yield stress during cycling, respectively, and a is the crack length. Although the above equation is applicable to the small-scale yielding condition, we hypothesize that the cyclic

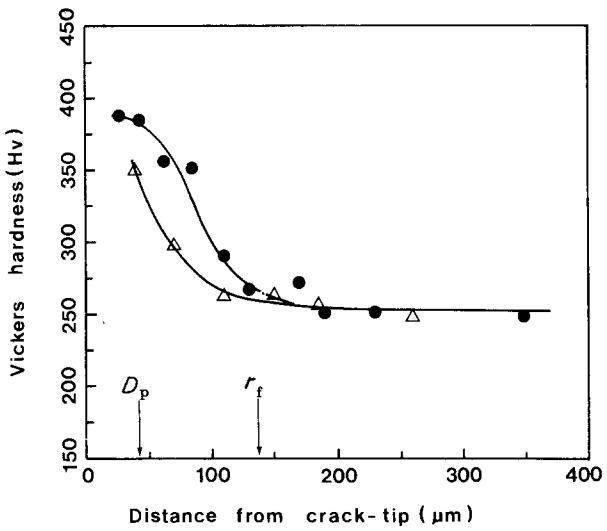

Figure 1 Microhardness profile ahead of fatigue crack cycled at 865 K under a total strain range of ± 2.0% for AISI 304L stainless steel. Crack length = 1 mm; (●) + 45° direction, (△) − 45° direction. The arrows are calculated results for the process zone (D_p) and cyclic plastic zone (r_f).

plastic zone size somewhat depends on the value of $(\Delta K/\sigma_{yc})^2$ even for the LCF regime. α_f is a characteristic constant which determine such dependency. Even though α_f depends on the specimen shape or yielding scale condition, it may be counted as a constant which is independent of the applied plastic strain range and temperature under the same specimen shape and LCF regime.

According to the plastic deformation characteristics at a fatigue crack tip suggested by Rice [20], in the small-scale yielding condition the distribution of stress and plastic strain in the cyclic plastic zone are determined by the following relations:

$$\sigma(r) \propto \left(\frac{1}{r}\right)^{n'/(n'+1)} \qquad (2)$$

$$\varepsilon(r) \propto \left(\frac{1}{r}\right)^{1/(n'+1)} \qquad (3)$$

where n' is the cyclic stress–strain exponent and r is the distance from the crack tip. Since the situation of concern to us is the high-strain LCF regime, the entire specimen is plastically deformed during the cycling. However, for straining above the yield point it can be assumed that the entire specimen including the crack tip region is work-hardened as a power law of the form $\sigma_T = k' \Delta\varepsilon_p^{n'}$, and the flow stress of the entire specimen is located on the elastic–plastic boundary during continuous deformation. If, then, the above HRR field can also be considered to be effective within the cyclic plastic zone in the post-yield condition of the high-strain LCF regime, then considering that the flow stress of the bulk is equal to the tensile peak stress, σ_T, caused by work hardening, Equation 2 becomes

$$\sigma(r) = \sigma_T \left(\frac{r_f}{r}\right)^{n'/(n'+1)} \qquad (4)$$

This flow stress distribution is depicted with respect to distance in Fig. 2. On the other hand, assuming that the stress level in the crack tip process zone (of size D_p)

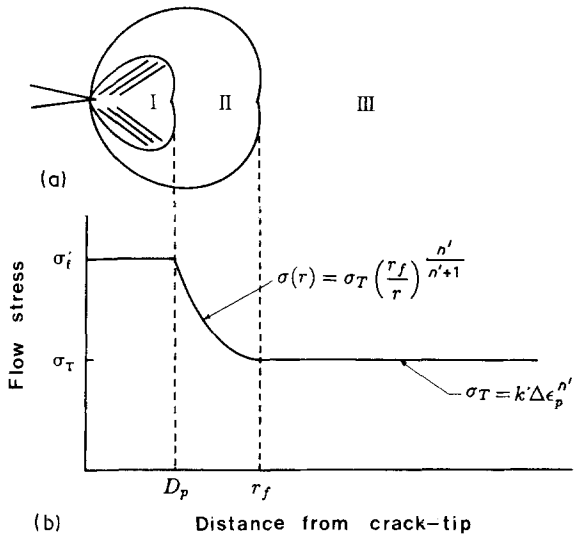

Figure 2 Idealized depiction of (a) fatigue crack-tip region and (b) its flow stress distribution. Region I: fatigue process zone, region II: cyclic plastic zone, region III: monotonic plastic zone.

approaches the ultimate tensile strength of a fatigued specimen, σ_f', arising from severe local shearing deformation, $\sigma(r)$ in Equation 4 maintains a constant value of σ_f' within the range from $r = 0$ to $r = D_p$. Therefore, the size of the process zone is suggested to be expressed by the relation

$$D_p = \alpha_f \left(\frac{\sigma_T}{\sigma_f'}\right)^{n'/(n'+1)} \left(\frac{\sigma_T}{\sigma_{yc}}\right)^2 a \quad (5)$$

The zone size in Equation 5 is shown to be increased with increasing n' and related to the ratio of σ_T to σ_f' and σ_{yc}.

As the stress intensification within the process zone is relieved at the expense of the local shearing deformation, a shearing process is continuously occurring and the total amount of accumulated strain in the zone is continuously increased during a tensile ramp while the stress is limited to a certain level. From Equation 3 for the plastic strain distribution adjacent to the crack tip, considering the boundary condition $\varepsilon = \Delta\varepsilon_p$ (plastic strain corresponding to the tensile peak stress, σ_T) at the cyclic plastic zone boundary ($r = r_f$), one can express the strain at any element of a material at a distance from the crack tip, r, in the cyclic plastic zone boundary during the loading part of the fatigue cycle, as

$$\varepsilon_p(r) = \Delta\varepsilon_p \left(\frac{r_f}{r}\right)^{1/(n'+1)} \quad (6)$$

The magnitude of the accumulated average strain in the process zone during a tensile ramp is obtained from the following concept of obtaining the average strain:

$$\varepsilon_p^{avg} = \frac{\int_0^{D_p} \varepsilon_p(r)\, dr}{D_p} = \frac{n'+1}{n'} \Delta\varepsilon_p \alpha_f^{1/(n'+1)} \left(\frac{\sigma_f'}{\sigma_{yc}}\right)^{2/(n'+1)} \times a^{1/(n'+1)} D_p^{-1/(n'+1)} \quad (7)$$

Tomkins [8] has proposed that the length of crack advance per cycle can be expressed by the externally applied strain multiplied by the flow band size as follows:

$$\frac{da}{dN} = \varepsilon_p D_p$$

But, actually, the process zone sustains a larger strain than the externally applied strain caused by the strain localization in the crack tip, and the crack advance will be related to this accumulated strain. Therefore, considering that the crack advance per cycle is determined by the amount of accumulated average strain in the process zone, the crack propagation rate can be expressed by replacing ε_p^{avg} instead of ε_p in the above equation

$$\frac{da}{dN} = \varepsilon_p^{avg} D_p \quad (8)$$

Substituting Equations 5 and 7 into Equation 8, the crack growth rate, da/dN, in the low-cycle fatigue regime can be given by the equation

$$\frac{da}{dN} = \alpha_f \frac{n'+1}{n'} \Delta\varepsilon_p \left(\frac{\sigma_T}{\sigma_{yc}}\right)^2 \left(\frac{\sigma_T}{\sigma_f'}\right) a \quad (9)$$

On integration, assuming that all the endurance of a specimen is taken up in the crack propagation and considering that σ_T and $\Delta\varepsilon_p$ are linked in a power law of the form $\sigma_T = k'\Delta\varepsilon_p^{n'}$, the endurance law is given by

$$\alpha_f \left(\frac{n'+1}{n'}\right) \frac{k'^3 \Delta\varepsilon_p^{3n'+1}}{\sigma_{yc}^2 \sigma_f'} = \frac{\ln(a_f/a_i)}{N_f} \quad (10)$$

where a_f and a_i are the final and initial crack size, respectively, and k' is the cyclic stress–strain coefficient. Equation 10 can be reduced to the Coffin–Manson law as follows:

$$N_f^{1/(3n'+1)} \Delta\varepsilon_p = \left[\frac{\ln(a_f/a_i)}{\alpha_f} \left(\frac{n'}{n'+1}\right) \frac{\sigma_{yc}^2 \sigma_f'}{k'^3}\right]^{1/(3n'+1)} \quad (11)$$

Comparing Equation 11 with the Coffin–Manson law ($N^{\alpha}\, \Delta\varepsilon_p$ is constant), the exponent $1/(3n'+1)$ turns out to be α while in Tomkins' model the exponent α value was found to be $1/(2n'+1)$, which was slightly overestimated as they indicated. For a given material, the constant α_f is determined as a unique value from one fatigue test result at any testing condition.

3. Results and discussion

The test specimen was a round type AISI 304L stainless steel whose diameter was 7 mm and gauge length 8 mm. The alloy, whose composition is shown in Table I, was solution-annealed at 1373 K for 1 h, aged at 1033 K for 50 h and water-cooled. Strain-controlled low-cycle fatigue tests with a strain rate of $4 \times 10^{-3}\ s^{-1}$ were carried out in an Ar atmosphere using a servo-hydraulic fatigue test machine. The results and parameters of LCF tests are listed in Tables II and III, respectively. The maximum crack tip flow stress, σ_f', is regarded as the ultimate tensile strength of the fatigued specimen to a half of total endurance and the cyclic yield strength, σ_{yc}, is regarded as the value corresponding to a strain of 0.2%

TABLE I Chemical composition of commercial and P-doped 304L stainless steel

Material	Composition (wt %)							
	C	Si	Mn	P	S	Cr	Mo	Ni
Commercial	0.025	0.37	1.48	0.026	0.018	18.04	0.42	10.1
P-doped	0.029	0.30	1.10	0.209	0.020	18.00	0.39	9.2

TABLE II Continuous LCF results at two temperatures of 304L stainless steel

Temperature (K)	$\pm \Delta\varepsilon_t$ (%)	$\Delta\varepsilon_p$ (%)	σ_T (MPa)	N_{cr}
823	2.5	2.62	314	401
	2.0	1.77	286	974
	1.5	1.21	250	1945
	1.0	0.66	198	7400
865	2.5	2.72	304	321
	2.0	2.03	280	485
	1.5	1.17	256	1202

TABLE III LCF parameters of AISI 304L stainless steel

Temperature (K)	n'	k'	σ_{yc} (MPa)	σ'_f (MPa)
823	0.34	1109	190	371
865	0.21	638	179	365

in the cyclic stress–strain relation. The initial crack length in Equation 11, a_i, is assumed to be 5 μm because in high-strain fatigue such a depth of crack is known to be comparatively early formed through the persistent slip-band and grain-boundary incompatibility [22, 23]. The final crack length, a_f, is considered to be 2 mm which is obtained from observation of the final rupture surface. Substituting the experimental data (N_f, n', k', σ_{yc}, σ'_f), obtained under the conditions of one temperature and a plastic strain range, into Equation 11 the characteristic material parameter, α_f, independent of temperature and plastic strain range, is obtained. For AISI 304L stainless steel, α_f is found to be 5.74×10^{-2} and with this value of α_f the fatigue lives are predicted from Equation 11 and the results are shown in Fig. 3. Surprisingly enough, the predicted values are in excellent agreement with the experimentally observed ones over a wide range of plastic strain.

To see if our model is valid for other materials such as 1Cr–Mo–V [24], AISI 4140 steel [25] and 12Cr–Mo–V [26], using the results of the fatigue tests and the parameters of these alloys listed in Table IV, a comparison of the predictions with the experimental results was conducted and the results are shown in Fig. 4. The predicted results for these alloys are found to be also in good agreement with the experimental ones. This good agreement for several materials may mean that our model is generally applicable.

Our theoretical development for the LCF endurance is similar to the existing models in that the

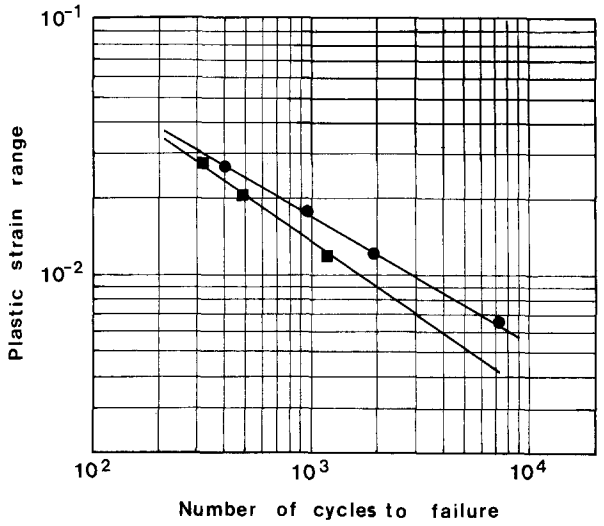

Figure 3 Coffin–Manson plots of experimental and predicted results for AISI 304L stainless steel at two testing temperatures: (●) 823 K [21], (■) 865 K, (——) model prediction. $4 \times 10^{-3} s^{-1}$, Ar (99.999%).

TABLE IV LCF parameters for three alloy systems

Alloy	n'	k'	σ_{yc} (MPa)	σ'_f (MPa)
1Cr–Mo–V	0.103	682	359	539
AISI 4140	0.106	1041	540	820
12Cr–Mo–V	0.110	525	265	412

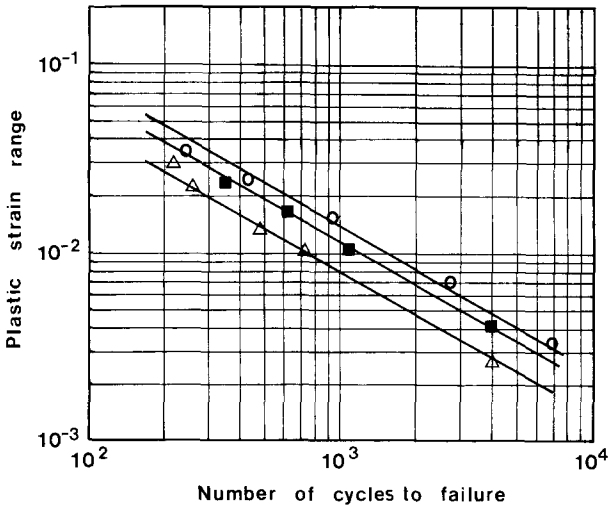

Figure 4 Coffin–Manson plots of experimental and predicted results for three alloys: (○) 1Cr–1Mo–0.25V, 823 K [24]; (■) AISI 4140 steel, 303 K [25]; (△) 12Cr–1Mo–0.25V, 873 K [26]; (——) model prediction. $4 \times 10^{-3} s^{-1}$, continuous cycling.

crack tip sliding-off process in the process zone is considered. However, our model has several characteristic concepts for the process zone which distinguish it from other suggestions.

Firstly, it has been reported by Saxena and Antolovich [13] that a high fatigue resistance is achieved by the large process zone size which induces a smaller strain intensification in the zone. In our model, however, a high fatigue resistance is related to a minimum product of the process zone size and the strain intensification in the zone which are reversely correlated

with each other through the cyclic stress–strain exponent, n' (see Equation 8). Therefore, to achieve high LCF resistance, both of these two factors must be limited to a small value at one time. This will be discussed later.

Secondly, the size of the developed process zone is quantitatively more reasonable than other suggestions, and this is consistent with the experimental results. For 304L stainless steel tested at 865 K and a total strain range of $\pm$ 2.0%, the process zone size, D_p, and cyclic plastic zone size, r_f, ahead of a crack length of 1 mm predicted from Equation 5 and Equation 1 have the values 42 and 139 μm, respectively. Fig. 1 shows the fatigue crack tip microhardness profile measured in the $\pm$ 45° directions with respect to the crack propagation direction for 304L stainless steel tested in the above-mentioned condition. For the measurement of the hardened matrix only, a carefully polished specimen was electro-etched so that grain boundary precipitates were removed from the surface. The observed zone sizes are in good agreement with the above predicted ones as denoted in Fig. 1. On the other hand, according to the result suggested by the Tomkins model [8], the extent of the process zone predicted from Equation 12 below has the value of 1 μm for 304L stainless steel under the test conditions of 865 K and $\Delta\varepsilon_t = \pm 2.0\%$

$$D_p = \left[\sec\left(\frac{\pi\sigma_T}{2T}\right) - 1\right]a \qquad (12)$$

where T is tensile strength.

According to the approach employed by Yokobori, the "appropriate length", s (which can be considered as the size of the process zone), in some cases, has a value greater than the monotonic zone size referred to by Bailon and Antolovich [7]. These two results are unreasonable compared with those of the present investigation and the considerations of many investigators [13, 14, 17, 27].

Thirdly, though our model for the process zone is based on continuum mechanics, it may reflect microstructural factors through the mechanical parameters. In general, it is believed that the process zone size is related to intrinsic microstructural factors. Davidson [14] has proposed that at near-threshold crack growth rates the length of the crack tip slip line (or process zone) is compatible with the mean free slip length or dispersoid spacing. Table V shows the predicted process zone size ahead of cracks of 1 mm cycled with a plastic strain range of $\pm$ 2.0% and at different temperatures. As compared with AISI 304L stainless steel, the three alloys 1Cr–Mo–V, AISI 4140 and 12Cr–Mo–V steel have smaller process zone sizes. Fig. 5a, b and c, observed from specimens cycled to half of the total endurance, show densely and finely distributed precipitates (cementite, carbide) while for aged AISI 304L stainless steel no precipitates are observed within the grains (Fig. 5d) but most of the precipitates exist along the grain boundaries. Therefore, partially, the small process zone size of the first three alloys in Table V may be attributed to the distribution of the precipitates which impedes the extension of the process zone ahead of the crack tip. On the other hand, for 304L stainless steel, the zone size is found to be nearly the same as the dimension of the grains because the impeding effect caused by the precipitates does not exist but comes only from grain boundaries.

TABLE V Theoretical process zone size, D_p, ahead of cracks of 1 mm cycled under a plastic strain range of $\pm$ 2.0% for different temperatures

Material	Process zone size (μm)
1Cr–Mo–V	11
AISI 4140	7
12Cr–Mo–V	19
AISI 304L	55
P-doped 304L	94

In addition to the precipitate effect, the proposed zone size may be affected by the stacking fault energy (SFE) effect. According to Saxena and Antolovich [13], it has been remarked that Al addition to Cu decreases the SFE and such an effect enlarges the crack tip process zone size because of the planar slip characteristics. In this work, to observe the effect of SFE, a P-doped 304L stainless steel [28] was compared with the commercial 304L stainless steel. The addition of P reduced the SFE by the effect of Suzuki segregation of P in 304L stainless steel as shown in previous work [28]. Table VI shows the parameters obtained from fatigue tests at 823 K. Table V and Fig. 6 show the theoretical process zone size and a comparison between the predicted life and the experimental one, respectively. From these results, one can realize that the proposed model for the endurance predicts the reduced fatigue life very well in P-doped 304L with the same constant α_f, while the predicted process zone size in P-doped 304L stainless steel is nearly twice as large as that in commercial 304L.

These results for the process zone relation with SFE are consistent with the suggestion of Felter and Laird [29] and Saxena and Antolovich [13] that a decrease of SFE increases the size of the process zone. However, contrary to the report by Saxena and Antolovich [13] that a high fatigue resistance is achieved by a large process zone size which induces a smaller strain intensification in the zone, the experimental result for endurance shows that fatigue life of P-doped 304L stainless steel is shorter than that of commercial 304L. This can be explained with our model which can predict the reduced fatigue life in P-doped 304L. That is, in our model, a high fatigue resistance is related to a minimum value of the product of the process zone size and the amount of strain intensification in the zone which are reversely correlated with each other, and to achieve a high LCF resistance, both of these two factors must be limited to a small value at one time. Therefore, the reduced fatigue life in P-doped 304L is attributed to the large process zone size which does not effectively contribute to relaxation of the strain intensification. This can be identified with Equation 7 which shows similar zone sizes in both materials under the same conditions. From these considerations for the present model, it is believed that not only a large

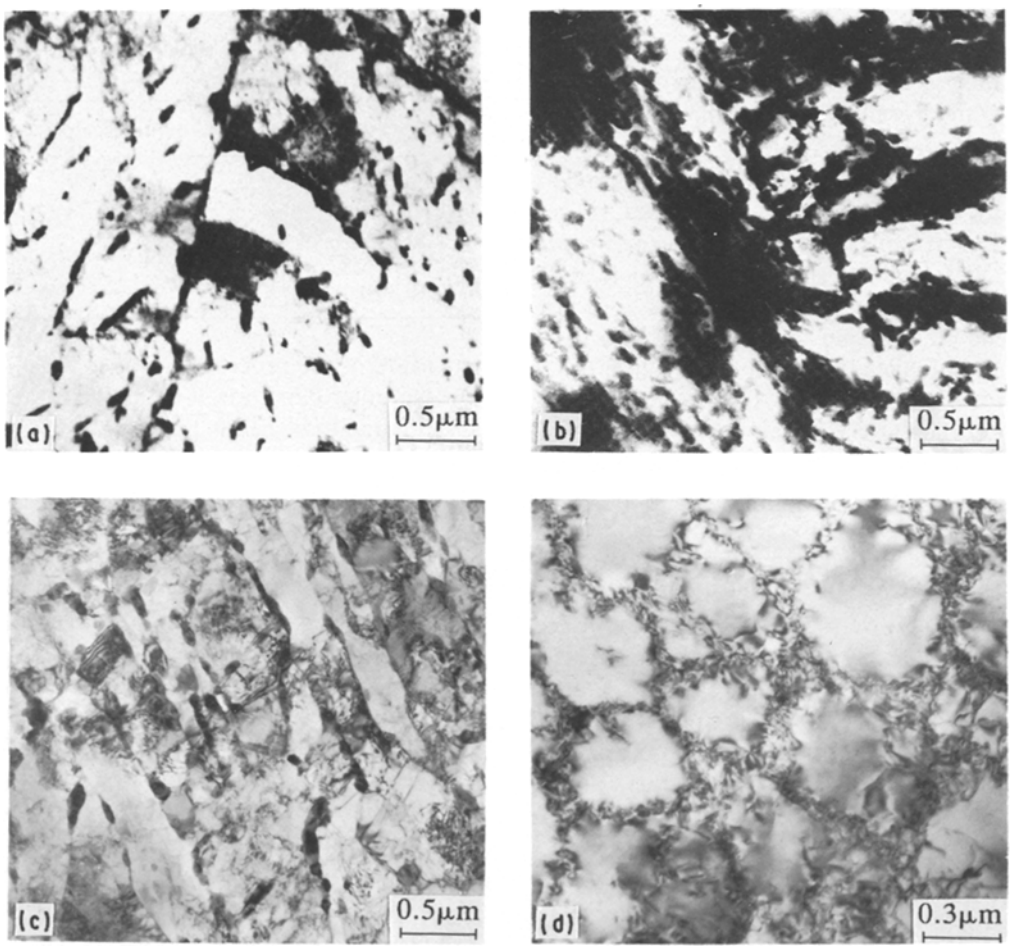

Figure 5 TEM micrographs of four alloy systems cycled at a total plastic strain range of ± 2.0%: (a) 1Cr–Mo–V at 823 K [24], (b) AISI 4140 steel at 300 K [25], (c) 12Cr–Mo–V at 873 K [26], (d) AISI 304L at 823 K.

TABLE VI LCF results and parameters for commercial and P-doped 304L stainless steel at 823 K

Material	n'	k'	σ_{yc} (MPa)	σ_f' (MPa)
AISI 304L	0.340	1109	190	371
P-doped 304L	0.245	933	196	412

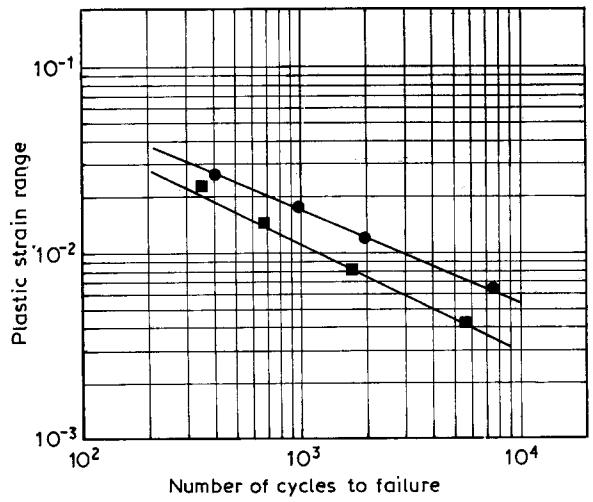

Figure 6 Coffin–Manson plots for (●) commercial [21] and (■) P-doped 304L stainless steel [28]; (——) model prediction. $4 \times 10^{-3}\,s^{-1}$, 823 K, Ar (99.999%).

process zone size which induces a smaller strain intensification is necessary for high fatigue resistance, but a decreasing rate of intensified strain with increase of the process zone is important; if the rate of decrease of the intensified strain is very low, then on the contrary the extended process zone induces an increase of the crack growth rate and a decrease of the fatigue life.

4. Conclusions

Our theoretical development of a model for continuous LCF crack advance and life prediction is characterized as follows.

1. In the LCF condition, the fatigue process zone within which the actual degradation of the material takes place is suggested as the region where the stress distribution of the HRR field approaches the maximum flow stress of the material, and this approach results in more correct features for the zone than previous work which has been based on a rough approximation.

2. Though the process zone size is formulated from continuum mechanics, it is compatible with metallurgical factors, i.e. precipitates and SFE.

3. According to our model, a higher fatigue resistance is related to a minimum product of process zone size and the strain intensification in the zone at the same time. That is to say, not only a smaller process

zone size but a smaller strain intensification is indispensable to obtain high fatigue resistance.

4. The Coffin–Manson exponent, α, obtained from our theoretical development, is suggested to have the value $1/(3n' + 1)$ and these results are in good agreement with not only 304L stainless steel but other materials in the low-cycle fatigue condition.

Acknowledgement

This work was financially supported by the Korea Advanced Institute of Science and Technology.

References

1. G. G. GARRETT and L. F. KNOTT, *Metall. Trans.* **7A** (1976) 883.
2. J. WAREING, *ibid.* **8A** (1977) 711.
3. B. TOMKINS and J. WAREING, *Met. Sci.* (1977) 414.
4. B. TOMKINS, *ibid.* (1980) 408.
5. C. LAIRD, in "Fatigue Crack Propagation", ASTM STP 415 (American Society for Testing and Materials, Philadelphia, 1967) p. 131.
6. P. NEUMANN, *Acta Metall.* **22** (1974) 1155.
7. J. P. BAILON and S. D. ANTOLOVICH, *ibid.* (1983) 313.
8. B. TOMKINS, *Phil. Mag.* **18** (1968) 1041.
9. J. WEERTMAN, in "Fatigue and Microstructure" (ASM, Metals Park, Ohio, 1979) p. 279.
10. T. YOKOBORI, S. KONOSU and A. T. YOKOBORI Jr, in Proceedings, "Fracture 1977", ICF4, Waterloo, Canada, edited by D. R. M. Taplin (1977) p. 665.
11. S. D. ANTOLOVICH, A. SAXENA and G. R. CHANANI, *Engng Fract. Mech.* **7** (1975) 649.
12. J. K. TIEN and S. PURUSHOTHAMAN, *Mater. Sci. Engng* **34** (1978) 2347.
13. A. SAXENA and S. D. ANTOLOVICH, *Metall. Trans. A* **6A** (1975) 1809.
14. D. L. DAVIDSON, *Acta Metall.* **32** (1984) 707.
15. C. LOYE, C. BATHIAS, D. RETALI and J. C. DEVAUX, in "Fatigue Mechanisms: Advances in Quantitative Measurement of Physical Damage", ASTM STP 811, edited by J. LANKFIRD, D. L. DAVIDSON, W. L. MORRIS and R. P. WEI (American Society for Testing and Materials, Philadelphia, 1983) p. 427.
16. C. Q. BOWLES and J. SCHIJVE, *ibid.* p. 400.
17. D. L. DAVIDSON and J. LANKFORD, *J. Engng Mater. Technol. Trans. ASME* (1976) 24.
18. C. BATHIAS and R. M. PELLOUX, *Metall. Trans.* **4** (1973) 1265.
19. C. E. JASKE, *Fatigue Engng Mater. Struct.* **6** (1983) 159.
20. J. R. RICE, in "Fatigue Crack Propagation", ASTM STP 415 (American Society for Testing and Materials, Philadelphia, 1967) p. 247.
21. S. C. LEE and S. W. NAM, *J. Korean Inst. Met.* **27** (1989) 32.
22. J. WAREING and H. G. VAUGHAN, *Met. Sci.* **11** (1977) 439.
23. J. C. GROSSKREUTZ, *J. Appl. Phys.* **33** (1962) 1787.
24. J. H. RYU, PhD thesis, Korea Advanced Institute of Science and Technology (1989).
25. I. S. CHOI, S. W. NAM and K.-T. RIE, *J. Mater. Sci.* **4** (1985) 97.
26. B. O. KONG and S. W. NAM, *J. Korean Inst. Met.* **29** (1991) 514.
27. J. AWATANI and T. SHIRAISHI, *Metall. Trans. A* **7A** (1976) 1599.
28. J. J. KIM and S. W. NAM, *Scripta Metall.* **23** (1989) 1473.
29. C. E. FELTER and C. LAIRD, *Acta Metall.* **15** (1967) 1621.

Received 2 July 1990
and accepted 2 August 1991